Fifth-order susceptibility unveils growth of thermodynamic amorphous order in glass-formers

S. Albert,[1] Th. Bauer,[2]* M. Michl,[2] G. Biroli,[3,4] J.-P. Bouchaud,[5] A. Loidl,[2]
P. Lunkenheimer,[2] R. Tourbot,[1] C. Wiertel-Gasquet,[1] F. Ladieu[1]†

Glasses are ubiquitous in daily life and technology. However, the microscopic mechanisms generating this state of matter remain subject to debate: Glasses are considered either as merely hyperviscous liquids or as resulting from a genuine thermodynamic phase transition toward a rigid state. We show that third- and fifth-order susceptibilities provide a definite answer to this long-standing controversy. Performing the corresponding high-precision nonlinear dielectric experiments for supercooled glycerol and propylene carbonate, we find strong support for theories based on thermodynamic amorphous order. Moreover, when lowering temperature, we find that the growing transient domains are compact—that is, their fractal dimension d_f = 3. The glass transition may thus represent a class of critical phenomena different from canonical second-order phase transitions for which d_f < 3.

The glassy state of matter, despite its omnipresence in nature and technology (*1*), continues to be one of the most puzzling riddles in condensed-matter physics (*1, 2*): For all practical purposes, glasses are rigid like crystals, but they lack any long-range order. Some theories describe glasses as kinetically constrained liquids (*3*), becoming so viscous below the glass transition that they seem effectively rigid. By contrast, other theories (*4, 5*) are built on the existence of an underlying thermodynamic phase transition to a state where the molecules are frozen in well-defined yet disordered positions. This so-called "amorphous order" cannot be revealed by canonical static correlation functions, but rather by new kinds of correlations [i.e., point-to-set correlations or other measures of local order (*6, 7*)] that have been detected in recent numerical simulations (*7–9*). In these theories, thermodynamic correlations lock together

the fluctuations and response of the molecules, which collectively rearrange over some length scale ℓ, ultimately leading to rigidity. In this thermodynamic scenario, ℓ is proportional to a power of $\ln(\tau_\alpha/\tau_0)$, where τ_α is the structural relaxation time and τ_0 is the microscopic time scale, generally smaller than 1 ps [4, 5]. Because equilibrium measurements require a time longer than τ_α, they cannot be performed in the range where ℓ is very large, which would require exponentially long times. This limitation is essentially why the true nature of glasses is still a matter of intense debate.

Here, we propose a strategy to unveil the existence of a thermodynamic length ℓ that grows upon cooling. Instead of only varying the temperature T, we also vary the nonlinear order k of the response of supercooled liquids. This is motivated by a general, although rarely considered [10], property of critical points: At a second-order critical temperature T_c, the linear susceptibility χ_1 associated with the order parameter is not the only diverging response. As a function of temperature, all the higher-order responses χ_{2m+1} ($m \geq 1$) diverge even faster than χ_1 itself. This comes from the fact that the divergences of all the χ_{2m+1} have the same origin—namely, the divergence of the length ℓ. By using the appropriate scaling theory, it can be shown that the larger the value of m, the stronger the divergence in temperature.

[1]SPEC, CEA, CNRS, Université Paris-Saclay, CEA Saclay Bat 772, 91191 Gif-sur-Yvette Cedex, France. [2]Experimental Physics V, Center for Electronic Correlations and Magnetism, University of Augsburg, 86159 Augsburg, Germany. [3]IPhT, CEA, CNRS, Université Paris-Saclay, CEA Saclay Bat 774, 91191 Gif-sur-Yvette Cedex, France. [4]LPS, Ecole Normale Supérieure, 24 rue Lhomond, 75231 Paris Cedex 05, France. [5]Capital Fund Management, 23 rue de l'Université, 75007 Paris, France. *Present address: Institute for Machine Tools and Industrial Management, Technical University of Munich, 85748 Garching, Germany. †Corresponding author. Email: francois.ladieu@cea.fr
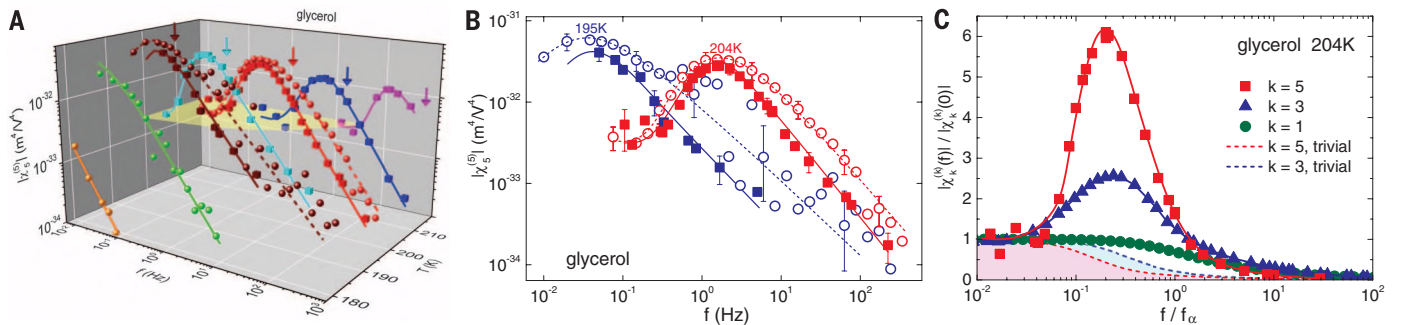
As theoretically shown below, transposing this idea to glasses requires taking into account that the putative "amorphous" or hidden order in supercooled liquids [7, 11] is not reflected in χ_1 itself, but only in higher-order response functions χ_{2m+1} ($m \geq 1$). This idea is indeed supported by previous measurements and analyses of the third-order susceptibility χ_3 [12–16]. We report results on the fifth-order susceptibility $\chi_5(T)$ and compare them to $\chi_3(T)$ in two canonical glass forming-liquids, glycerol and propylene carbonate. If critical phenomena really play a key role for the glass transition, χ_5 should increase much faster than χ_3 as the liquid becomes more viscous.

This scenario can be understood by means of a theoretical argument based on previous work [17] and further detailed in [18]. Suppose that $N_{corr} = (\ell/a)^{d_f}$ molecules are amorphously ordered over the length scale ℓ, where a is the molecular size and d_f is the fractal dimension of the ordered clusters. This implies that their dipoles, oriented in apparently random positions, are essentially locked together during a time τ_α. We expect that in the presence of an external electric field E oscillating at frequency $\omega \geq \tau_\alpha^{-1}$, the dipolar degrees of freedom of these molecules contribute to the polarization per unit volume as

$$p = \mu_{dip} \frac{\sqrt{(\ell/a)^{d_f}}}{(\ell/a)^d} F\left[\frac{\mu_{dip}E\sqrt{(\ell/a)^{d_f}}}{kT}\right] \quad (1)$$

where μ_{dip} is an elementary dipole moment, F is a scaling function such that $F(-x) = -F(x)$, and $d = 3$ is the dimension of space. This states that randomly locked dipoles have an overall moment $\sim \sqrt{N_{corr}}$ and that we should compare the energy of this "super-dipole" in a field to the

thermal energy. Equation 1 is motivated by general arguments involving multipoint correlation functions through which d_f can be given a precise meaning [18] and is fully justified when ℓ diverges, in particular in the vicinity of a critical point such as the mode-coupling transition or the spin-glass transition. In the latter case, Eq. 1 is in fact equivalent to the scaling arguments of [19], provided one performs suitable mapping between the magnetic formalism of [19] and ours.

Expanding Eq. 1 in powers of E, we find the "glassy" contribution to p:

$$\frac{p}{\mu_{dip}} = F'(0)\left(\frac{\ell}{a}\right)^{d_f-d}\left(\frac{\mu_{dip}E}{kT}\right)$$
$$+ \frac{1}{3!}F^{(3)}(0)\left(\frac{\ell}{a}\right)^{2d_f-d}\left(\frac{\mu_{dip}E}{kT}\right)^3$$
$$+ \frac{1}{5!}F^{(5)}(0)\left(\frac{\ell}{a}\right)^{3d_f-d}\left(\frac{\mu_{dip}E}{kT}\right)^5 + \ldots \quad (2)$$

Because d_f must be less than or equal to d, we find that the first term, contributing to the usual linear dielectric constant $\chi_1(\omega)$, cannot grow as ℓ increases. This simple theoretical argument explains why we do not expect spatial glassy correlations to show up in $\chi_1(\omega)$. The second term, contributing to the third-order dielectric constant, does grow with ℓ, provided $d_f > d/2$. Although $d_f < d$ close to a standard second-order critical point [20] such as the spin-glass transition, several theories suggest [4, 5, 21, 22] that ordered domains are compact ($d_f = d$), in which case $(\ell/a)^{2d_f-d} = (\ell/a)^d = N_{corr}$, as assumed in our previous work [17, 23]. The third term of Eq. 2 reveals that the fifth-order susceptibility $\chi_5(\omega)$ should diverge as ℓ^{3d_f-d}. Therefore, the joint measurement of $\chi_3(\omega)$ and $\chi_5(\omega)$ provides a direct way to estimate d_f

Fig. 1. Modulus of the fifth-order susceptibility in supercooled glycerol measured with two independent setups. (**A**) The susceptibilities $\chi_5^{(5)}$ reported here are obtained directly [18] by monitoring the response of the sample at 5ω when applying an electric field E at angular frequency ω. Two independent setups were used, designed either to maximize the field amplitude (Augsburg setup, spheres) or to optimize the sensitivity (Saclay setup, cubes). Lines are guides to the eye. Errors are on the order of the scatter of neighboring data points around the lines. Both setups yield consistent results. For a given temperature T, $|\chi_5^{(5)}|$ has a humped shape, with a maximum occurring at the frequency $f_{peak} \approx 0.22 f_\alpha$ where f_α is the relaxation frequency indicated by a colored arrow for each temperature. When decreasing T, the height of the hump increases strongly. The yellow plane emphasizes the fact that, for a given T, $\chi_5^{(5)}$ is constant for $f/f_\alpha \leq 0.05$. (**B**) Projection onto the susceptibility-frequency plane of the data in Fig. 1A at 204 K and at 195 K. The agreement around and below the peak is remarkable at 204 K (see text). The relative evolution of the height of the peak is reasonably similar between 204 K and 195 K for the two setups (see Fig. 3A). (**C**) Comparison of the fifth-order, cubic, and linear susceptibilities of glycerol [the latter is notated $\chi_1^{(1)}$ for convenience [18]]. Symbols, with lines to guide the eye, are Saclay data at 204 K; the error bars are on the order of the size of the symbols for $k = 5$ [except at the lowest frequencies [18]] and smaller for $k = 3$ and 1. The higher the order k, the stronger the hump of $|\chi_k^{(k)}|$; this is a key result supporting the amorphous-order scenario. The dashed lines, emphasized by colored areas, correspond to the trivial response of an ideal gas of dipoles without amorphous order. In this case, $|\chi_k^{(k)}|$ decreases monotonously in frequency for any value of k. The higher k, the stronger the difference between the measured and trivial susceptibility.

experimentally through the following relation:

$$|\chi_5| \propto |\chi_3|^{\mu(d_f)}; \ \mu(d_f) = \frac{3d_f - d}{2d_f - d}; \ d_f(\mu) = d\frac{\mu - 1}{2\mu - 3}$$

$$(3)$$

where the exponent $\mu(d_f)$ is equal to 2 when the dynamically correlated regions are compact ($d_f = d$), and is higher otherwise. We predict two key results that can be obtained from χ_5 and χ_3 susceptibility measurements. First, if amorphous order increases approaching the transition, the frequency dependence should be more anomalous [i.e., more humped (18)] for $\chi_5(\omega)$ than for $\chi_3(\omega)$. Second, the growth of χ_5 should be much stronger than that of χ_3 when lowering the temperature, following $\chi_5 \sim \chi_3^2$ if we assume compact amorphous domains. Our work provides experimental evidence that these predictions indeed hold and suggests that the glass transition represents a new type of critical phenomenon with growing length and time scales but with $d_f = d$, in contrast to the spin-glass transition that instead displays (19) canonical critical behavior with $d_f \approx 2.35$.

We measured $\chi_5(\omega)$ in glycerol and propylene carbonate by applying a field of amplitude E and frequency $f = \omega/(2\pi)$ (18). The fifth-order response is $\propto \chi_5 E^5$ and is orders of magnitude smaller than the cubic and linear ones, given by $\propto \chi_3 E^3$ and $\propto \chi_1 E$, respectively. We avoided any contributions of χ_3 and of χ_1 by measuring the signal at 5ω, which only contains the component $\chi_5^{(5)}$ of the fifth-order susceptibility (18). We measured $\chi_5^{(5)}$ with two independent setups because of the very small amplitude, optimized along complementary strategies. One setup (in Augsburg) was designed to achieve the highest possible field (reaching 78 MV/m). We optimized sensitivity with a differential technique using two samples of different thicknesses in the other setup (Saclay; see fig. S1), which required lower fields (up to 26 MV/m).

We obtained the values of $|\chi_5^{(5)}(\omega)|$ for glycerol at various frequencies and temperatures by using the two aforementioned techniques (Fig. 1A). A clear peak arises for a given T in $|\chi_5^{(5)}(\omega)|$ for a frequency $f_{peak} \approx 0.22f_\alpha$ where the α-relaxation frequency f_α, defined by the peak of the out-of-phase linear susceptibility, is indicated by arrows in Fig. 1A. Even though the data were determined by two independent setups, the overall agreement is remarkable (Fig. 1B). The most accurate comparison is possible at 204 K, where f_{peak} is well inside the frequency range accessible by the two setups. The two spectra at 204 K coincide on the low-frequency side of the peak (18). On the other side of the peak, a discrepancy between the two sets of data progressively increases with frequency, reaching a constant factor of 4 at the highest frequencies (Fig. 1B). Apart from the value of the electric field, the main difference between the two experiments is the number of applied field cycles n. The Saclay setup measured the stationary responses ($n \to \infty$), whereas n remained finite in the Augsburg setup [similarly to (24)], ranging from $n = 2$ at the lowest frequencies to $n \propto f$ at the highest frequencies. The two setups give the same results for $\chi_5^{(5)}$ because at sufficiently low values of f/f_α, the response of
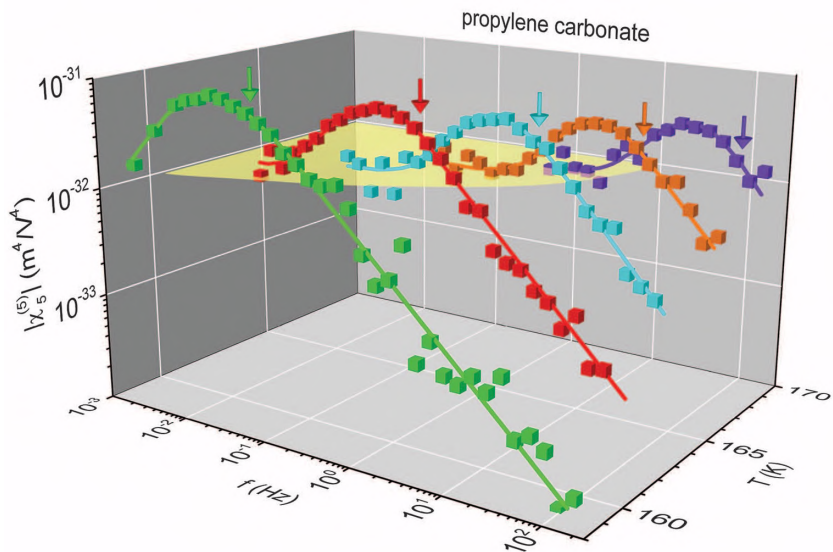

Fig. 2. Modulus of the fifth-order susceptibility in supercooled propylene carbonate. The experimental data (symbols) were obtained with the Augsburg setup. The presentation of the graph is analogous to Fig. 1A to emphasize the similarity of the behavior of $|\chi_5^{(5)}|$ in propylene carbonate and in glycerol, even though these two liquids have different fragilities and different types of intermolecular interactions (van der Waals bonding versus hydrogen bonding).

the supercooled liquid is likely to instantaneously follow the field. By contrast, at higher frequencies $\omega \gtrsim \tau_\alpha^{-1}$, the finite cycle number may play a role, making a quantitative treatment of this effect difficult (18). Our further analysis relies on the behavior of the peaks of $\chi_5^{(5)}$, and more precisely on their relative evolution with temperature, which reasonably agrees in the two setups (see below).

The qualitative features of $|\chi_5^{(5)}(\omega)|$ (Fig. 1, A and B) are reminiscent of those of the third-harmonic cubic susceptibility $|\chi_3^{(3)}(\omega)|$ (12, 13). Both quantities exhibit a humped shape, with a peak located at the same frequency $f_{peak} \approx 0.22f_\alpha$, as well as a strong increase of the height of the peak as the temperature is decreased. These two distinctive features are important because they are specific signatures of glassy dynamical correlations (17), in contrast to trivial systems without correlations (25). In this case, the modulus of all higher-order nonlinear susceptibilities monotonously decreases with frequency (18, 25).

To quantitatively compare the frequency dependency of the susceptibilities $\chi_k^{(k)}$ of order k, we plotted $|\chi_k^{(k)}(f/f_\alpha)/\chi_k^{(k)}(0)|$ of glycerol for $k = 5$, 3, and 1 ($\chi_1^{(1)}$ is the linear susceptibility noted χ_1 above) (Fig. 1C). The peak amplitude for $k = 5$ is strongly enhanced relative to $k = 3$—that is, the higher the nonlinear order k, the more anomalous the frequency dependence (Fig. 1C and figs. S2 and S3). This behavior is a decisive result and is fully consistent with our scaling analysis. For archetypical glass-formers, we can always fit the linear susceptibility by assuming a sum of Debye relaxations where $\chi_{1,Debye} \propto 1/(1 - i\omega\tau)$. We do this by choosing a suitable distribution $G(\tau)$ of relaxation times τ (26) caused by dynamical heterogeneities. Because the trivial response discussed above also obeys $\chi_{1,trivial} \propto 1/(1 - i\omega\tau)$,

we have used (18, 25) the same distribution $G(\tau)$ to calculate the trivial responses $\chi_{k,trivial}^{(k)}$ for $k = 3$ and 5. For a given $k > 1$, a large difference exists between the experimental spectrum of $|\chi_k^{(k)}(f/f_\alpha)/\chi_k^{(k)}(0)|$ and its trivial counterpart (Fig. 1C), which we can ascribe to correlation-induced effects. For $k = 1$, the experimental data agree with the trivial response [convoluted with $G(\tau)$], consistent with the theoretical arguments stating that glassy correlations do not change the linear response (17). For $k = 3$ and 5, the difference to the trivial response increases, being much more important for $k = 5$, where it exceeds one order of magnitude. This quantitatively supports the scaling prediction obtained assuming that collective effects due to the growth of amorphous order play a key role in supercooled liquids.

We measured $|\chi_5^{(5)}(\omega)|$ at five different temperatures for propylene carbonate (Fig. 2). Propylene carbonate differs from glycerol in that its fragility $(27, 28)$ $m \propto [\partial \log(\tau_\alpha)/\partial(1/T)]_{T_g}$ (where T_g is the glass transition temperature) is twice as large and it has van der Waals bonding, in contrast to hydrogen bonding. Despite these differences, the anomalous hump-like features of glycerol (Fig. 1A) are also observed in propylene carbonate (Fig. 2). We expect this behavior from our scaling framework, which relies on the predominant role of collective dynamical effects in supercooled liquids. The presence of similar anomalous features in two very different glass-formers suggests that they only weakly depend on the specific microscopic properties of the material.

To elicit the temperature dependence of collective effects, we introduced dimensionless quantities related to $\chi_3^{(3)}$ and $\chi_5^{(5)}$:

$$X_3^{(3)} \equiv \frac{k_B T}{\varepsilon_0 \Delta\chi_1^2 a^3}\chi_3^{(3)}, \qquad X_5^{(5)} \equiv \frac{(k_B T)^2}{\varepsilon_0^2 \Delta\chi_1^3 a^6}\chi_5^{(5)} \quad (4)$$
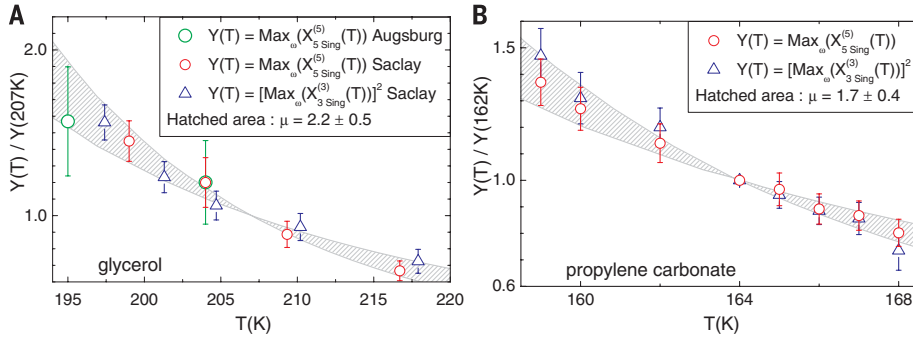
Fig. 3. Comparison of the temperature dependence of the singular part of the fifth-order and cubic dimensionless susceptibilities at f_{peak}. (**A**) For glycerol, the singular part of $|X_k^{(k)}(f_{\text{peak}})|$ for $k = 3$ and 5 is normalized to 1 at 207 K. The value of the exponent μ is then determined by comparing $|X_{5,\text{sing}}^{(5)}(f_{\text{peak}})|$ to $|X_{3,\text{sing}}^{(3)}(f_{\text{peak}})|^{\mu}$; the symbols for $k = 3$ correspond to $\mu = 2$, and the hatched area shows the interval corresponding to the error bar given for μ (*18*). The two Augsburg data points for $X_5^{(5)}$ have been added on the graph by scaling to the Saclay point at 204 K; the Augsburg point at 195 K is reasonably well within the hatched area, which shows that the relative evolution of $X_5^{(5)}$ with temperature is consistent in the two setups. (**B**) Same display as in (A), but for propylene carbonate with $T = 164$ K as the normalization temperature and the symbols for $k = 3$ corresponding to $\mu = 2$.

where ε_0 is the permittivity of free space, $\Delta\chi_1 = \chi_1(0) - \chi_1(\infty)$ is the dielectric strength, a^3 is the molecular volume, and k_B is the Boltzmann constant. The main advantage of these dimensionless nonlinear susceptibilities is that in the trivial case of an ideal gas of dipoles, both $X_{3,\text{trivial}}^{(3)}$ and $X_{5,\text{trivial}}^{(5)}$ are independent of temperature when plotted versus scaled frequency (*18*, *25*). Hence, we ascribe their experimental variation to the nontrivial dynamical correlations in the supercooled liquid (*17*, *23*). This interpretation is strongly supported by previous findings (*12–14*, *23*) where the temperature dependence of $|X_3^{(3)}|$ was studied at various values of f/f_α. Close to and above its peak frequency, $|X_3^{(3)}|$ was found to strongly vary in temperature, contrary to the low-frequency plateau region ($f/f_\alpha \leq 0.05$) where $|X_3^{(3)}|$ no longer depends on temperature. This low-frequency region corresponds to time scales much longer than τ_α where the liquid flow destroys glassy correlations, making each molecule effectively independent of others and yielding a dielectric response close to the aforementioned trivial case. This is why, to determine the temperature evolution of the glassy dynamical correlations, we focused on the region of the peak of $|\chi_5^{(5)}|$. For each of the two liquids, this peak appears at the very same frequency f_{peak} as in $|\chi_3^{(3)}|$.

We expect the nonlinear susceptibilities to contain a trivial contribution that would exist even for independent dipoles, as well as a "singular" contribution (i.e., diverging with ℓ) as given in Eq. 2. We thus write

$$X_{3,\text{sing}}^{(3)} \equiv X_3^{(3)} - X_{3,\text{trivial}}^{(3)}, \qquad X_{5,\text{sing}}^{(5)} \equiv X_5^{(5)} - X_{5,\text{trivial}}^{(5)} \tag{5}$$

Here, the trivial contributions are calculated by assuming a set of independent Debye dipoles convoluted with the aforementioned distribution $G(\tau)$ of relaxation times (*18*). We compared the temperature evolution of $|X_{5,\text{sing}}^{(5)}[f_{\text{peak}}(T)]|$ and that of $|X_{3,\text{sing}}^{(3)}[f_{\text{peak}}(T)]|^{\mu}$ (Fig. 3) to derive

the value of the exponent μ, from which we deduce the fractal dimension d_f of the dynamically correlated regions by using Eq. 3. In both glycerol and propylene carbonate, the value $\mu = 2$, corresponding to compact domains of dimension $d_f = 3$, is found to be consistent with experiments (triangles in Fig. 3). By fitting the T dependence of $|X_{3,\text{sing}}^{(3)}[f_{\text{peak}}(T)]|$ with a smooth function (*18*), we found the hatched area corresponding to $\mu = 2.2 \pm 0.5$ in glycerol and $\mu = 1.7 \pm 0.4$ in propylene carbonate (Fig. 3). The fact that, within experimental uncertainty, a value of $\mu \approx 2$ is common to each of the two liquids supports a picture of amorphous compact domains mostly independent of differences at the molecular level and validates the correlation length scale for our scaling analysis. Considering that the temperature interval in Fig. 3B is smaller by a factor of 2, we note that the critical behavior in propylene carbonate is stronger than in glycerol (Fig. 3A). This suggests that the larger the fragility, the stronger the temperature dependence of the thermodynamic length ℓ. This is easily understood in the scenario of (*4*), where the critical point is the Vogel-Fulcher temperature T_0: In this case, equilibrium measurements can be made closer to the critical point for more fragile liquids, because the larger the fragility, the smaller the difference between T_g and T_0.

Our experimental results are therefore consistent with the general predictions of theories such as the random first-order transition or frustration-limited domains (*4*, *5*), where the physical mechanism driving the glass transition is of thermodynamic origin and where some nontrivial (albeit random) long-range correlations build up between molecules. Only in this case (*18*) can one have N_{corr} dipolar degrees of freedom collectively responding over some length scale ℓ and over time scales on the order of τ_α. If instead the glass transition is regarded as a purely dynamical phenomenon, there would not be any anomalous increase of the normalized peak value of the higher-order

susceptibilities at all (*18*). Our results therefore severely challenge theories advocating against any thermodynamic signature and favoring purely dynamic scenarios. Moreover, from a comparison of the higher-order susceptibilities, our results are consistent with $\chi_5 \propto \chi_3^2$. This constitutes evidence for compact amorphously ordered domains (i.e., $d_f = d$) pointing toward a nonstandard nature of the glass transition, in contrast to canonical second-order phase transitions for which $d_f < d$.

REFERENCES AND NOTES

1. M. D. Ediger, P. Harrowell, *J. Chem. Phys.* **137**, 080901 (2012).
2. L. Berthier, G. Biroli, *Rev. Mod. Phys.* **83**, 587–645 (2011).
3. D. Chandler, J. P. Garrahan, *Annu. Rev. Phys. Chem.* **61**, 191–217 (2010).
4. M. Dzero, J. Schmalian, P. G. Wolynes, in *Structural Glasses and Supercooled Liquids: Theory, Experiment, and Applications*, P. G. Wolynes, V. Lubchenko, Eds. (Wiley, 2012), pp. 193–222.
5. G. Tarjus, S. A. Kivelson, Z. Nussinov, P. Viot, *J. Phys. Condens. Matter* **17**, R1143–R1182 (2005).
6. S. Mossa, G. Tarjus, *J. Chem. Phys.* **119**, 8069 (2003).
7. G. Biroli, J.-P. Bouchaud, A. Cavagna, T. S. Grigera, P. Verrocchio, *Nat. Phys.* **4**, 771–775 (2008).
8. R. Pinney, T. B. Liverpool, C. P. Royall, *J. Chem. Phys.* **143**, 244507 (2015).
9. L. Berthier, P. Charbonneau, S. Yaida, *J. Chem. Phys.* **144**, 024501 (2016).
10. Y. Kimura, S. Hara, R. Hayakawa, *Phys. Rev. E* **62**, R5907–R5910 (2000).
11. J.-P. Bouchaud, G. Biroli, *J. Chem. Phys.* **121**, 7347–7354 (2004).
12. C. Crauste-Thibierge *et al.*, *Phys. Rev. Lett.* **104**, 165703 (2010).
13. T. Bauer, P. Lunkenheimer, A. Loidl, *Phys. Rev. Lett.* **111**, 225702 (2013).
14. C. Brun, F. Ladieu, D. L'Hôte, G. Biroli, J.-P. Bouchaud, *Phys. Rev. Lett.* **109**, 175702 (2012).
15. U. Buchenau, R. Zorn, M. A. Ramos, *Phys. Rev. E* **90**, 042312 (2014).
16. R. Casalini, D. Fragiadakis, C. M. Roland, *J. Chem. Phys.* **142**, 064504 (2015).
17. J.-P. Bouchaud, G. Biroli, *Phys. Rev. B* **72**, 064204 (2005).
18. See supplementary materials on *Science* Online.
19. L. P. Lévy, *Phys. Rev. B* **38**, 4963–4973 (1988).
20. A. Coniglio, A. Fierro, in *Encyclopedia of Complexity and Systems Science*, R. A. Meyers, Ed. (Springer, 2009), pp. 1596–1615.
21. J. D. Stevenson, J. Schmalian, P. G. Wolynes, *Nat. Phys.* **2**, 268–274 (2006).
22. G. Biroli, J.-P. Bouchaud, in *Structural Glasses and Supercooled Liquids: Theory, Experiment, and Applications*, P. G. Wolynes, V. Lubchenko, Eds. (Wiley, 2012), pp. 31–114.
23. F. Ladieu, C. Brun, D. L'Hôte, *Phys. Rev. B* **85**, 184207 (2012).
24. R. Richert, S. Weinstein, *Phys. Rev. Lett.* **97**, 095703 (2006).
25. W. T. Coffey, B. V. Paranjape, *Proc. R. Irish Acad. A* **78**, 17–25 (1978).
26. T. Blochowicz, C. Tschirwitz, S. Benkhof, E. A. Rössler, *J. Chem. Phys.* **118**, 7544–7555 (2003).
27. P. G. Debenedetti, F. H. Stillinger, *Nature* **410**, 259–267 (2001).
28. R. Böhmer, K. L. Ngai, C. A. Angell, D. J. Plazek, *J. Chem. Phys.* **99**, 4201–4209 (1993).